Birmingham's air and surface urban heat islands associated with Lamb weather types and cloudless anticyclonic conditions

Zhang, Fang; Cai, Xiaoming; Thornes, John

DOI:
10.1177/0309133314538725

Citation for published version (Harvard):
Zhang, F, Cai, X & Thornes, J 2014, 'Birmingham's air and surface urban heat islands associated with Lamb weather types and cloudless anticyclonic conditions', *Progress in Physical Geography*, vol. 38, no. 4, pp. 431-447. https://doi.org/10.1177/0309133314538725

Birmingham's air and surface urban heat islands associated with Lamb weather types and cloudless anticyclonic conditions

Abstract

This study investigates the characteristics of the air and surface urban heat islands (aUHI and sUHI) of Birmingham in relation to Lamb weather types (LWTs) over the period 2002-2007, with a particular focus on cloudless anticyclonic conditions. Ground-based MIDAS air temperatures within urban canopy layer at the urban Edgbaston and rural Shawbury weather stations were used to derive the aUHI intensity (aUHII). Satellite-derived MODIS/Aqua land surface temperatures (LST) under cloudless conditions were used to derive the spatial patterns of the sUHI as well as the sUHI intensity (sUHII). Using Jenkinson's objective daily synoptic indices, a combined subset of eleven LWTs were examined for their association with the nocturnal aUHII. Over the study period, the most frequently occurring LWT, 'anticyclonic' (21.1%), gives a strongest mean/maximum nocturnal aUHII of 2.5 ℃/7 ℃ (391 nights) and the largest proportion of nocturnal heat island events of 65.2%. The spatial patterns of nocturnal sUHI for each LWT were also assessed, and the results showed that Birmingham's sUHI spatial patterns demonstrate Birmingham's urban warming of up to 4.16 ℃ (48 clear nights) in the city centre under cloudless anticyclonic conditions. The scatter plot of nocturnal aUHII and sUHII for the 48 nights demonstrates a linear aUHI-sUHI relationship. We also developed a simple analytical model that links the slope of the aUHI-sUHI relationship to the difference of "built-up" area fraction between the urban pixel and the rural pixel. This partially explains the physical basis behind the relationship. These findings of aUHII-sUHII relationships may lead to a future development of a generic methodology of deriving the spatial patterns of aUHI from satellite measurement.

Keywords: Lamb weather types; anticyclonic; urban heat island; air temperature; MODIS; land surface temperature; Birmingham

1. Introduction

During the 20th century, the urban population of England increased from 77% to 89% (Hicks and Allen, 1999). With rapid urbanisation and climate change (IPCC, 2007) increased urban warming is likely to trigger more issues of urban health and wellbeing. Due to the thermal properties of construction materials, lack of vegetation, ‘urban canyons’ and anthropogenic heat (Smith et al., 2009), the excess heat absorbed during the daytime causes warmer nights, contributing to higher urban temperatures than those in surrounding rural areas. This phenomenon is referred to as the urban heat island (UHI) effect, which generally refers to warmer air temperatures, but refers to warmer surface temperatures as well (Voogt, 2000). It is well known that the UHI is more prominent on calm and clear summer nights (Oke, 1987). The UHI impacts can be beneficial, particularly the reduced winter mortality and reduced road salting due to less icy roads (Voogt, 2000). However, the summer UHI in warmer cities is generally adverse to human health as it can cause additional heat stress in hot weather. The significance of the UHI on heatwaves for cities was highlighted in August 2003 when London’s UHI intensity reached up to 6 to 9 ℃, causing nearly 600 excess deaths (Mayor of London, 2006). In Birmingham, there was a significant UHI effect of over 4.5 ℃ during the 2006 heatwave (Tomlinson et al., 2012a).

To identify the UHI, previous studies have used either direct or indirect measurement methods. Air urban heat island (aUHI) can be quantified from air temperature (T_{air}) directly measured by weather monitoring stations (within the urban canopy layer). Long-term trends in London’s aUHI have been examined by Lee (1992), Jones and Lister (2009) and Wilby et al. (2011). Wilby (2003) projected London’s future UHI using the Met Office HadCM3 climate model. Unfortunately, the UKCP09 projections are not able to predict the future UHI due to the missing contribution from urban surfaces in regional climate models (Wilby et al., 2009). Surface urban heat island (sUHI) can be quantified using land surface temperatures (LST) indirectly measured by satellite remote-sensing. Remote-sensing measures radiances in various wavelength bands that are used to estimate surface temperatures. The satellite images do derived for clear-sky conditions capture the spatial views of urban surface temperature (i.e. the skin temperature). Satellite-derived studies have been limited in low-resolution sensors such as 1.1 km pixels for Advanced Very High Resolution Radiometer (AVHRR) (Roth et al., 1989) and 1 km for the Moderate Resolution Imaging Spectroradiometer (MODIS) (Wan et al., 2004). There have been very few thermal studies with high spatial resolution using Landsat-5 Thematic Mapper (TM) (Liu and Zhang, 2011) and Landsat-7 Enhanced Thematic Mapper Plus (ETM+) (120 m for TM and 60 m for ETM+) due to limited temporal coverage and the infrequent cloudless weather conditions. In recent years, the MODIS instrument operating on the National Aeronautics and Space Administration (NASA)’s Aqua and Terra satellite sensors has been widely used for LST measurements and sUHI studies (Hung et al., 2006). Both satellites can view the entire surface of the Earth every 1-2 days and acquire data in 36 spectral bands at three spatial resolutions of 250 m (Band 1-2), 500 m (Band 3-7) and 1000 m (Band 8-36) (MODIS, http://modis.gsfc.nasa.gov/). In addition, not all bands are available at the three spatial resolutions. The MODIS LST at 5 km resolution is retrieved in bands 20, 22, 23, 29 and 31-33. For the clear sky pixels, the LST is retrieved in bands 31 and 32 at 1 km resolution (Wan et al., 2004) with the generalized split-window algorithm (Wan and Dozier 1996). For a given time and location, different satellite images will be generated using Aqua- and Terra-MODIS sensors based on their different orbits. Tomlinson et al. (2012a) derived Birmingham's summer nocturnal sUHI for different Pasquill-Gifford stability classes (Pasquill and Smith, 1983) using MODIS/Aqua LST data. The specific case study for 2006 heatwave event found a Birmingham sUHI peak of 4.88 ℃.

Lamb weather types (Lamb, 1950, 1972), LWTs, have been used to classify synoptic airflow circulations based on the pressure patterns for the British Isles. There have been very few UHI studies undertaken in relation to synoptic weather types such as that by Unwin (1980) for Birmingham, showing that mean nocturnal aUHI peaked at 1.34 K in autumn (10 September-19 November) during 1965-1974. Anticyclonic circulation was associated with a maximum mean nocturnal aUHI intensity of 2.26 K, and cyclonic circulation was associated with a minimum mean nocturnal aUHI intensity of 0.49 K. Morris and Simmonds (2000) examined the relationship between the UHI magnitude and anomalous synoptic conditions in Melbourne, Australia. These studies suggested that anticyclonic conditions favour the development of the aUHI (and by inference the sUHI). In addition, it should be noted that the frequency of LWTs vary with location, for example, London is more dominated by anticyclonic, easterly and southerly weather types than Birmingham due to its relatively continental location (O'Hare et al., 2005).

There have been some studies into the comparison of satellite-derived LST with ground-based T_{air} (Hachem et al., 2012; Tomlinson et al., 2012b; White-Newsome et al., 2013; Jin and dickinson, 2010), but very few on the comparison of aUHI and sUHI. Considering the lack of combined research of aUHI and sUHI in relation to LWTs, this study builds upon Unwin (1980)'s synoptic methods to examine Birmingham's nocturnal aUHI and follows the technical methods of Tomlinson et al. (2012a) using MODIS/Aqua images to assess Birmingham's nocturnal sUHI. The authors also notice the scarce of investigation of the aUHII-sUHII relationship, which is practically important because this relationship will pave the way for the development of a generic methodology of deriving the spatial patterns of aUHI from satellite measurement. This relationship will be examined in this study for cloudless anticyclonic nights in Birmingham.

2. Data and methods

2.1 Study area

The West Midlands region is located in western central England. It contains the UK's second most populous city (Birmingham), and a county, which includes seven metropolitan boroughs. It covers 13,004 km^2 with a population of 5,602,000. Birmingham covers 268 km^2 with a population of 1,073,000 (ONS, 2011). The UK Met Office is trying to select ideal stations which could represent wider area around the station and not unduly affected by local effects i.e. ground level station without vegetation and buildings (Met Office, 2011). Indeed, it is impossible to find a perfect weather station. In this study, two weather stations, Edgbaston and Shawbury (Figure 1), located in the West Midlands were selected as the urban and rural stations, respectively. The Edgbaston station (52.476°N, -1.934°W) is located in Birmingham's central area approximately 2 km from the city centre at an elevation of 160 m. The Shawbury station (52.795°N, -2.665°W) is located approximately 65 km to north-west of Edgbaston at an elevation of 72 m. The selection of urban/rural stations is mainly based on their locations and surrounding environments (see Section 2.2, Figure 2). The effects of elevation difference on the UHI calculation have been discussed by Jones and Lister (2009) and Peterson and Owen (2005). Here, the 88 m elevation difference between the Edgbaston and Shawbury stations is not taken directly into account in this study, but will be mentioned where appropriate. In addition, the Coleshill station located approximately 4.5 km to Birmingham's eastern edge is only used for obtaining the cloud cover data, which are not available at the Edgbaston station.

2.2 Land surface temperatures

The MODIS sensor is carried on both Aqua and Terra satellite platforms. Nocturnal satellite images obtained from the MODIS/Aqua satellite sensor pass over Birmingham at approximately 01:30 UTC local time, but at approximately 10:30 UTC for Terra (Tomlinson et al., 2012a). The MODIS product, *MYD11A1–MODIS/Aqua Land Surface Temperature/Emissivity (LST/E) Daily L3 Global 1 km SIN Grid V005* was used in this study. This dataset is available from 8th July 2002 up to the present with 1 km spatial resolution. Indeed, the 1 km grid is more precisely 0.93 km due to the errors caused by geo-location or satellite sensor observations (Wan, 2007). The data were obtained through the NASA Land Processes Distributed Active Archive Centre (LP DAAC) Data Pool. According to the MODIS Sinusoidal grid tiling system, the tile identifier of h17v03 was chosen to acquire the data across Birmingham.

The 1 km^2 pixels covering the urban Edgbaston and rural Shawbury are shown in Figure 2 and the locations of the weather stations are also marked. The Edgbaston station is surrounded by urban and built-up areas, mainly covered with buildings, vegetation (trees and parks) and a small part of a reservoir. By contrast, the Shawbury station is surrounded by a large proportion of grassland (or arable land) with a few clusters of low density buildings.

2.3 Air temperatures

Ground-based meteorological data comprised of hourly T_{air} at the Edgbaston and Shawbury stations, and cloud cover at the Coleshill station were obtained from the Met Office Integrated Data Archive System (MIDAS) Land Surface Stations data held at the British Atmospheric Data Centre (BADC). The data were extracted between 8th July 2002 and 31st July 2007 (2002-2007), coinciding with the period of data availability of the MODIS LST. In addition, the MIDAS T_{air} is measured at the screen height, and for the Edgbaston (urban) station, T_{air} is measured within the urban canopy layer. Daily maximum and minimum air temperature ($T_{air/max}$ and $T_{air/min}$) were derived from the hourly T_{air}; thus the time at which $T_{air/max}$ (or $T_{air/min}$) occurred may vary from day to day. In Section 3.3.1 where T_{air} is compared with LST, according to the acquisition time of satellite images at about 01:30 UTC, the meteorological variables averaged at 01:00 UTC and 02:00 UTC were used.

2.4 Lamb weather types

Lamb (1972) originally classified daily synoptic weather conditions based on the variations in surface pressures over the British Isles (50 - 60 °N, 2 °E - 10 °W). The following classifications of LWTs are included in the analysis: eight directional types (South-easterly [SE], Southerly [S], Northerly [N], Westerly [W], South-westerly [SW], North-westerly [NW], Easterly [E] and North-easterly [NE]), two non-directional types (Anticyclonic [A], Cyclonic [C]), and one Unclassified [U] type which represents days with weak or chaotic circulation patterns (Hulme and Barrow, 1997). Jenkinson and Collinson (1977) improved an objective LWTs using daily grid point mean sea-level pressure data, to classify daily circulation patterns into twenty-seven categories (including the LWTs, hybrid types recognised by Lamb (1972)). Similar to Unwin (1980), this study used the original eleven LWTs. Jenkinson's objective daily synoptic indices from 1st January 1880 to 31st July 2007 were downloaded from the Climatic Research Unit, University of East Anglia (http://www.cru.uea.ac.uk/). These indices were generated based on the dominant airflow direction and vorticity (O'Hare et al., 2005). Considering the data availability of Jenkinson's objective daily synoptic indices till 31st July 2007 and the data availability of the MODIS LST from 8th July 2002, the analysis of this study is performed over the period from 8th July 2002 to 31st July 2007, a total of 1850 days. During the study period, the days are associated with the original eleven LWTs account for approximately 73.6% of total days. The remaining hybrid types (anticyclonic-related ANE, AE, ASE, AS, ASW, AW, ANW and AN; cyclonic-related CNE, CE, CSE, CS, CSW, CW, CNW and CN) accounting for 26.4% of the total days are not discussed in this study.

2.5 Methods

The UHI intensity (UHII) in this study is defined as the temperature difference between the Edgbaston (urban) station and the Shawbury (rural) station. To examine the characteristics of Birmingham's UHIs (aUHI and sUHI), both ground-based MIDAS T_{air} and satellite-derived MODIS LST were analysed. To define a heat island event, a threshold value was selected for daily $T_{air/min}$. Days with nocturnal aUHI intensity (aUHII) in excess of 1.5 ℃ can be regarded as UHI events (Unwin, 1980). A value of 5 ℃ was chosen as a threshold for extreme UHI events. Nocturnal aUHII were grouped by LWT and Analysis of Variance (ANOVA) was conducted. The downloaded MODIS Scientific Data Set (SDS) in Hierarchical Data Format (HDF) with sinusoidal grid projections were converted to ArcGIS raster format using the Marine Geospace Ecology Tools (MGET)'s Convert SDS in HDF to ArcGIS Raster tool (Roberts et al., 2010). Once the LST images were converted to ArcInfo Binary Grid format, the spatial patterns were thereafter mapped by combining the outputs with Birmingham's shapefile obtained from EDINA Digimap (http://digimap.edina.ac.uk/boundary/). For the LWTs analysis, the MODIS satellite images were selected if they met the following three criteria: (i) complete pixel coverage of nocturnal LST across Birmingham, (ii) clear-sky conditions (0-okta cloud cover), and (iii) no unrealistically extreme high/low LST values. It is obvious that clouds may considerably affect the quality of satellite LST measurements. A total of 77 nocturnal images matched the three criteria. Among the 77 nights, 48 nights belong to LWT [A] type, 2 nights to [C], 9 nights to [SW], 2 nights to [W], 4 nights to [NW], 3 nights to [S], 2 nights to [N], 3 nights to [SE], 2 nights to [U], 1 night to [E] and 1 night to [NE]. To obtain the spatial patterns of Birmingham's sUHI for each LWT, the MODIS LST images for that LWT were averaged by using ArcGIS Map Algebra - Raster Calculator. To obtain the sUHI intensity (sUHII), ArcGIS Zonal Statistics - Spatial Analyst was performed to derive the LST from the urban Edgbaston station and the rural Shawbury station. In addition, the spatial patterns of sUHII were defined by subtracting the LST value retrieved at Shawbury from the 2-D LST.

3. Results and discussion

3.1 Ground-based aUHI

3.1.1 Variations of aUHI

Figure 3 represents the monthly variations of aUHII for the period 2002-2007 (N = 1850); error bars refer to the 95% Confidence Interval (CI) based on the standard error estimates of the sample means. The results show consistently stronger nocturnal aUHI intensities than daytime aUHI intensities for all seasons (spring: MAM; summer: JJA; autumn: SON; winter: DJF). In the period from May to August, the daytime aUHI intensities are positive. Statistical analysis of daytime aUHII provides an annual mean value of -0.2 ℃. The negative values of daytime aUHII from October to April (or November, January and February, if the elevation correction is made) imply an urban cold island and likely attributed to urban shading. Due to the study core of heat islands, the weak (or absent) daytime aUHI will not be discussed further.

Table 1 lists the seasonal mean values and standard deviations of nocturnal aUHII, and the numbers of heat island events together with extreme heat island events over 1850 days. Among four seasons, mean nocturnal aUHII is at a maximum in summer (1.7 ℃) and at a minimum in winter (0.8 ℃). In view of this, the aUHI is most prominent for summer nights but weakest in winter. This is because heat absorbed during the daytime is highest in summer and lowest in winter. During the study period, there was an average of 39.8% (N = 737) heat island events and 3.0% (N = 58) extreme heat island events. Heat island events most commonly occurred in summer (47.7%), followed by autumn (43.5%) and spring (39.3%), and least commonly occurred in winter with a proportion of 28.2%. Extreme heat island events mainly occurred in spring (3.9%) and summer (3.7%).

3.1.2 Nocturnal aUHI by LWT

Unwin (1980) analysed Birmingham's aUHI using Edgbaston as urban station and Elmdon as rural station, and classified the data into LWTs for a period of 1965-1974. In this study, a similar analysis is conducted for the West Midlands using the data detailed in Section 2.4.

Table 2 shows the summary of nocturnal aUHII, total numbers of nights and (extreme) UHI events for each LWT. Type [A], [C], [SW] and [W] have been recognised as the most commonly occurring weather types for UHI, having 21.1%, 11.7%, 9.4% and 8.7%, respectively. The results are consistent with the findings of O'Hare et al. (2005) who found that the top three most frequent weather types are [A], [W] and [C] accounting for approximately 50% of total days over the British Isles. Unlike Unwin (1980)'s findings that [W] (22.3%) and [A] (18.4%) were top two most frequently occurring types during 1965-1974, for our study period 2002-2007, [A] covered the highest frequency percentage of 21.1% but [W] only covered 8.7%. Unwin (1980) also found that [C] was associated with least nocturnal UHI effect (0.49 K), our results show that [C] was associated with a mean nocturnal aUHII of 0.9 ℃ which is higher than [N], [NE] and [E]. The 9.4% in frequency of [SW] is more than doubled compared to Unwin (1980)'s frequency percentage of 3.9%. The most dominant LWT, [A], was associated with a mean nocturnal aUHII of 2.5 ℃, the largest proportion of 65.2% of UHI events and 12.0% of extreme UHI events among all LTWs, and the maximum aUHII of 7 ℃. Two least dominant LWTs, [NE] and [E], were associated with mean nocturnal aUHII of 0.7 ℃ and 0.6 ℃, respectively. Although the LWT of [U] had low frequency, its mean nocturnal aUHII reached 2.2 ℃. During the 30 [U] days, approximately 60% (17 days) occurred in summer. For many other LWTs, [C] is positively skewed peaking at 'no UHI effect' aUHII of 0. The results of one-way ANOVA analysis confirm that the eleven LWTs explain the significant fraction of the variance in aUHI ($p < 0.01$), the excluded hybrid LWTs are statistically insignificant ($p > 0.05$).

It should be noted that, if a systematic difference in temperature between the two sites caused by factors other than land use is considered (Peterson and Owen, 2005), for example, the climatological temperature lapse rate due to the difference in elevation, interpretations throughout the section may be slightly altered. If a climatological lapse rate of temperature of 6°C km^{-1} is used, aUHII would be 0.53°C higher since the elevation of the Edgbaston site is 160 m and that of the Shawbury site is 72 m. In other words, the UHII calculated from the direct temperature measurements at the two sites underestimates the true UHII. If this correction were taken, the horizontal line of 'aUHII = 0' in Figure 3 would be moved down to the location of -0.53°C (as indicated by the dashed line) and equivalently all values of aUHII should be increased by 0.53°C.

3.2 Satellite-derived sUHI

Figure 4 shows the averaged spatial patterns of Birmingham's sUHII calculated from MODIS/Aqua nocturnal LST for each LWT, indicating Birmingham's urban warming relative to the surrounding rural areas. The number at the lower-right corner of each image is the number of nights to be averaged. A 'concentric pattern' is found in Birmingham central areas with sUHII decreasing towards the sub-urban or rural areas, particularly when influenced by [A], [SW] and [S] types. Birmingham's urban warming of up to 4.16 ℃ has been detected under the influence of [A] type in Fig. 4 [A]. It must be noted that this UHII of 4.16 ℃ is the averaged value of 48 nights and this pixel is not the one covering the Edgbaston station. In Section 3.3 we will show that the averaged sUHII for the pixel of Edgbaston is 3.0 ℃, lower than this maximum value of 4.16 ℃. Heat islands induced by [SE], [C] and [U] types can also be recognised but at a relatively weak level. Results highlight the significance of [A] type in dominating Birmingham's sUHI. Unfortunately for some LWTs ([C], [W], [N], [U], [NE] and [E]), only a small number of nights satisfied the three criteria and thus interpretation of the results should be made with caution.

3.3 Comparison of aUHI and sUHI for cloudless anticyclonic conditions

Because T_{air} is directly measured from a single-point weather station but LST is indirectly measured using satellite remote sensing at the 1 km^2 pixel spatial resolution, interpretation of the comparison between T_{air} and LST should be made cautiously. In principle, the LST reading of a pixel can be interpreted as an aggregated temperature of all upward-facing surfaces that the satellite sensor 'sees' (e.g. roads, roofs, tree tops, vegetation covers, etc.) inside the pixel. For an urban Edgbaston station shown in Figure 2(a), whereas T_{air} is the air temperature inside the urban canopy layer, the LST obtained from the MODIS/Aqua sensor may be influenced by rapidly cooled exposed surfaces, such as park areas, tree tops and even water bodies (reservoir, lake, etc.).

In this section, nocturnal LST and T_{air} at 01:30 UTC of the 48 cloudless anticyclonic nights at both the Edgbaston and Shawbury stations are analysed. In Figure 5, the averaged nocturnal LST and T_{air} for each month are plotted together with the averaged aUHII (01:30 UTC) and sUHII; also plotted as bars are the number of cloudless anticyclonic nights of each month. It is shown that the spring season (Mar-May) has the highest number of cloudless anticyclonic nights, whilst the winter season (Nov-Jan) has the lowest number. The highest sUHI is 5.9 ℃ occurred on 2 September 2002 and the highest aUHI is 6.8 ℃ occurred on 11 April 2007 (not shown). Figure 5 also shows that, although LST and T_{air} follow the normal seasonal pattern, UHI intensities do not vary significantly across the seasons. By excluding those months with only one or two nights (Jan, Aug, Oct, Nov, and Dec), we notice a difference of sUHII between summer months and spring months (i.e. higher in summer), but this difference is not as significant for aUHII. Mean aUHII for all 48 nights is 3.4 ℃, which is slightly higher than the mean sUHII of 3.0 ℃ by 0.4 ℃.

Figure 5 illustrates that for both stations, T_{air} is normally higher than LST (with only one exception of Shawbury in November). For the urban site this may be attributed to the fact that LST is influenced by the cold exposed surfaces of the pixel; for the rural site, however, nighttime radiation inversion could be the explanation of the warmer T_{air} than LST. Figure 6 (a) and (b) demonstrate the correlations between T_{air} and LST of all 48 nights for the two stations, respectively. The intercepts at LST=0 ℃ are interpreted as the difference between T_{air} and LST if the regression line has the slope of unity: 2.2 ℃ for the Edgbaston site and 1.6 ℃ for the Shawbury site. The slope of the regression line for Shawbury is indeed about 1, suggesting that the lower LST due to radiation cooling is independent season. On the other hand, the slope of the regression line for Edgbaston is 0.96, suggesting that the difference between T_{air} and LST is weakly season-dependent, reduced from 2.2 ℃ at LST=0 ℃ to 1.4 ℃ LST=20 ℃. For each station, nocturnal T_{air} and LST are strongly correlated at the 0.01 significance level ($r > 0.98$ for Edgbaston, $r > 0.97$ for Shawbury, $p < 0.01$).

The scatter plot of nocturnal aUHII and sUHII for the 48 nights is shown in Figure 6 (c), together with the linear regression results. The correlation is statistically significant at the 0.01 level (r = 0.419, $p < 0.01$) and accounted for approximately 18% of the variance of aUHII ($R^2 = 0.175$). The linear relationship between sUHI and aUHI can be explained by a simple analytical model as described in Box 1. This model is derived from a few assumptions which are reasonably justifiable. The model is expressed by Equation (8) in Box 1:

$$\text{aUHII} = \frac{1}{\alpha} \cdot \text{sUHI}$$

which implies that aUHII and sUHII are linearly related with a slope of $1/\alpha$, where $\alpha = \Delta f^{(b)}$ is the difference of “built-up” area fraction between the urban pixel and the rural pixel. Referring to Figure 2, $\Delta f^{(b)}$ is positive due to a greater coverage of urban “built-up” landuse type for the Edgbaston pixel than that for the Shawbury pixel. Although this model explains the linear relationship between sUHII and aUHII, the magnitude of the slope is larger than that in Figure 6. We attribute this mismatch to the inaccuracy of the assumptions. One example is the inaccuracy of Equation (6) in Box 1, as we know that under cloudless conditions, normally $\mathrm{T}_{\mathrm{air}(r)} > \mathrm{T}^{(o)}$ due to radiation inversion (as discussed earlier). This assumption replaces $\mathrm{T}^{(o)}$ (a lower value) in Equation (4) by $\mathrm{T}_{\mathrm{air}(r)}$ (a larger value) and causes a smaller $(\mathrm{T}^{(b)} - \mathrm{T}^{(o)})$. To compensate this, the coefficient α in Equation (7) should be larger, consequently leading to a smaller slope of $1/\alpha$. These findings of aUHII-sUHII relationships may lead to a future development of deriving the spatial patterns of aUHI using satellite-derived thermal images.

4. Conclusions

This study investigated the relationship between aUHII and sUHII (derived from ground-based T_{air} at two weather stations and satellite-sensed LST, respectively) in relation to Lamb weather types (LWTs) over the period 2002-2007 for Birmingham, UK, with a particular focus on cloudless anticyclonic conditions. Over the study period, the most frequently occurring (391 nights, 21.1% of 1850 nights) LWT, ‘anticyclonic’, gives a strongest mean (or maximum) nocturnal aUHII of 2.5 ℃

(or 7 ℃) and the largest proportion of nocturnal heat island events of 65.2% in this LWT. Among the selected 48 cloudless anticyclonic nights, the majority occurred in the spring and summer seasons and both aUHII and sUHII do not vary significantly across the seasons. The averaged sUHII and aUHII over the 48 nights are 3.0 ℃ and 3.4 ℃, respectively. T_{air} is normally higher than LST by about 1.4-2.2 ℃. The scatter plot of nocturnal aUHII and sUHII for the 48 nights demonstrates a linear aUHII-sUHII relationship. We also developed a simple analytical model that links the slope of the aUHII-sUHII relationship to the difference of "built-up" area fraction between the urban pixel and the rural pixel. This partially explains the physical basis behind the relationship.

In June 2011, two new weather stations were installed: one at the University of Birmingham (Winterbourne 2) and one at Paradise Circus in Birmingham city centre (the Edgbaston weather station has now closed). These two new stations are expected to provide more relevant urban weather data and better information for further research on Birmingham's UHI and the effect of climate change on extreme weather events. Since the UHI phenomenon describes the local-scale (regional) urban warming, the UHII calculated from different pairs of urban-rural stations could produce different UHI effects. Wan et al. (2002) raised an issue of the impact of rural station selection on UHII estimation. For the future research, more urban and rural weather stations will be considered to compare the UHI effect.

References

Hachem, S., Duguay, C.R. and Allard, M. (2012) Comparison of MODIS-derived land surface temperatures with ground surface and air temperature measurements in continuous permafrost terrain. **The Cryosphere**, 6: (1): 51-69.

Hicks, J. and Allen, G. (1999) "A Century of Change: Trends in UK statistics since 1900". SOCIAL AND GENERAL STATISTICS SECTION. HOUSE OF COMMONS LIBRARY.

Hulme, M. and Barrow, E. (1997) *Climate of the British Isles: present, past and furture*, Routledge, London, 454pp

Hung, T., Uchihama, D., Ochi, S., et al. (2006) Assessment with satellite data of the urban heat island effects in Asian mega cities. **International Journal of Applied Earth Observation and Geoinformation**, 8: (1): 34-48.

IPCC (2007) "Climate change 2007 : impacts, adaptation and vulnerability : contribution of Working Group II to the Fourth Assessment Report of the Intergovernmental Panel on Climate Change / edited by Parry, M.L. et al". Cambridge, Cambridge University Press.

Jenkinson, A.F. and Collinson, B.P. (1977) **An initial climatology of gales over the North Sea**.

Jin, M., Dickinson, R.E. (2010) Land surface skin temperature climatology: benifiting from the strengths of satellite observations. **Environmental Research Letters**, 5, 044004

Jones, P.D. and Lister, D.H. (2009) The urban heat island in Central London and urban-related warming trends in Central London since 1900. **Weather**, 64: (12): 323-327.

Lamb, H.H. (1950) Types and Spells of Weather around the Year in the British-Isles - Annual Trends, Seasonal Structure of the Year, Singularities. **Quarterly Journal of the Royal Meteorological Society**, 76: (330): 393-438.

Lamb, H.H. (1972) **British Isles weather types and a register of the daily sequence of circulation patterns, 1861-1971**. London: H.M.S.O.

Lee, D.O. (1992) URBAN WARMING?— AN ANALYSIS OF RECENT TRENDS IN LONDON'S HEAT ISLAND. **Weather**, 47: (2): 50-56.

Liu, L. and Zhang, Y.Z. (2011) Urban Heat Island Analysis Using the Landsat TM Data and ASTER Data: A Case Study in Hong Kong. **Remote Sensing**, 3: (7): 1535-1552.

Mayor of London (2006). London's Urban Heat Island: A Summary for Decision Makers. King's College London, ARUP, London School of Hygiene and Tropical Medicine, University of Birmingham, Brunel University, Arizona State University. London, UK

Met Office (2011) Weather stations. Available at : http://www.metoffice.gov.uk/learning/science/first-steps/observations/weather-stations

Morris, C.J.G. and Simmonds, I. (2000) Associations between varying magnitudes of the urban heat island and the synoptic climatology in Melbourne, Australia. **International Journal of Climatology**, 20: (15): 1931-1954.

O'Hare, G., Sweeney, J. and Wilby, R.L. (2005) **Weather, climate, and climate change : human perspectives / Greg O'Hare, John Sweeney and Rob Wilby**. Harlow: Prentice Hall.

Oke, T.R. (1987) **Boundary layer climates / T.R. Oke**. 2nd.London: Methuen.

ONS (2011) Office for National Statistics. Available at: http://www.ons.gov.uk/ons/index.html

Pasquill, F. and Smith, F.B. (1983) **Atmospheric diffusion**. 3rd / F. Pasquill and F.B. Smith.Chichester: Ellis Horwood.

Peterson, T.C. and Owen, T.W. (2005) Urban Heat Island Assessment: Metadata Are Important. **Journal of Climate**, 18: (14): 2637-2646.

Roberts, J.J., Best, B.D., Dunn, D.C., et al. (2010) Marine Geospatial Ecology Tools: An integrated framework for ecological geoprocessing with ArcGIS, Python, R, MATLAB, and C++. **Environmental Modelling & Software**, 25: (10): 1197-1207.

Roth, M., Oke, T.R. and Emery, W.J. (1989) Satellite-derived urban heat islands from three coastal cities and the utilization of such data in urban climatology. **International Journal of Remote Sensing**, 10: (11): 1699-1720.

Smith, C., Lindley, S. and Levermore, G. (2009) Estimating spatial and temporal patterns of urban anthropogenic heat fluxes for UK cities: the case of Manchester. **Theoretical and Applied Climatology**, 98: (1-2): 19-35.

Tomlinson, C.J., Chapman, L., Thornes, J.E., et al. (2012a) Derivation of Birmingham's summer surface urban heat island from MODIS satellite images. **International Journal of Climatology**, 32: (2): 214-224.

Tomlinson, C.J., Chapman, L., Thornes, J.E., et al. (2012b) Comparing night-time satellite land surface temperature from MODIS and ground measured air temperature across a conurbation. **Remote Sensing Letters**, 3 (8): 657-666.

Unwin, D.J. (1980) THE SYNOPTIC CLIMATOLOGY OF BIRMINGHAM'S URBAN HEAT ISLAND, 1965–74. **Weather**, 35: (2): 43-50.

Voogt, J.A. (2000) "Urban Heat Island". In Douglas, I. (Ed.) **Encyclopedia of Global Environmental Change: Causes and Consequences of Global Environmental Change**. Wiley-Blackwell 660-666.

Wan, Z. (2007) MODIS Land Surface Temperature products user' guide. Institute for Computational Earth System Science, University of California, Santa Barbara, CA, available at: http://www.icess.ucsb.edu/modis/LstUsrGuide/MODIS_LST_products_Users_guide_C5.pdf

Wan, Z. and Dozier, J. (1996) A generalized split-window algorithm for retrieving land surface temperature from space. **IEEE Transactions on Geoscience and Remote Sensing**, 34: 892-905

Wan, Z., Zhang, Y., Zhang, Q., et al. (2002) Validation of the land-surface temperature products retrieved from Terra Moderate Resolution Imaging Spectroradiometer data. **Remote Sensing of Environment**, 83: (1–2): 163-180.

Wan, Z., Zhang, Y., Zhang, Q., et al. (2004) Quality assessment and validation of the MODIS global land surface temperature. **International Journal of Remote Sensing**, 25: (1): 261-274.

White-Newsome, J.L., Brines, S.J., Brown, D.G., et al. (2013) Validating satellite-derived land surface temperature with in situ measurements: a public health perspective. (1552-9924 (Electronic)).

Wilby, R., Betts, R. and McCarthy, M. (2009) UK Climate Projections science report: climate change projections - Annex 7: urban heat island effects. University of Loughborough & Met Office Hadley Centre.

Wilby, R.L. (2003) Past and projected trends in London's urban heat island. **Weather**, 58: (7): 251-260.

Wilby, R.L., Jones, P.D. and Lister, D.H. (2011) Decadal variations in the nocturnal heat island of London. **Weather**, 66: (3): 59-64.

List of Figures

Figure 1. Map of the West Midlands, UK showing the locations of weather stations (the dark inset boundary surrounding Edgbaston is the West Midlands metropolitan county)

(a) Urban

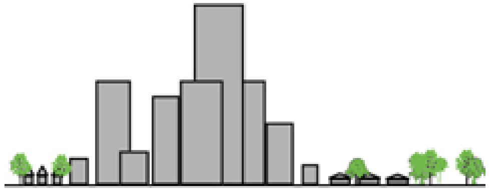

(b) Rural

Figure 2. Satellite images showing the surroundings of local weather stations: (a) Edgbaston and (b) Shawbury, corresponding to the MODIS 1 km^2 pixels

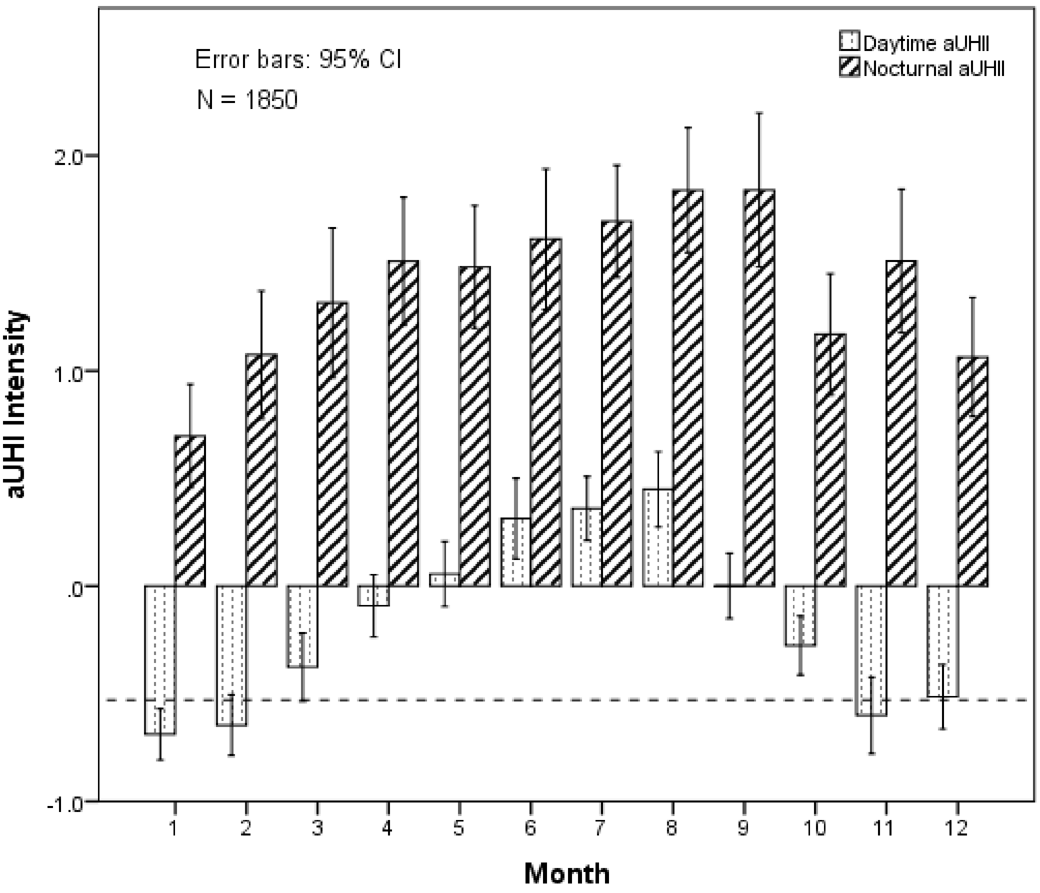

Figure 3. Monthly mean daytime and nocturnal aUHII at Edgbaston (urban) and Shawbury (rural) weather stations, 2002-2007 (the dashed line indicates the level of aUHII = 0 if a climatological temperature lapse rate of 6 ℃ km^{-1} were considered)

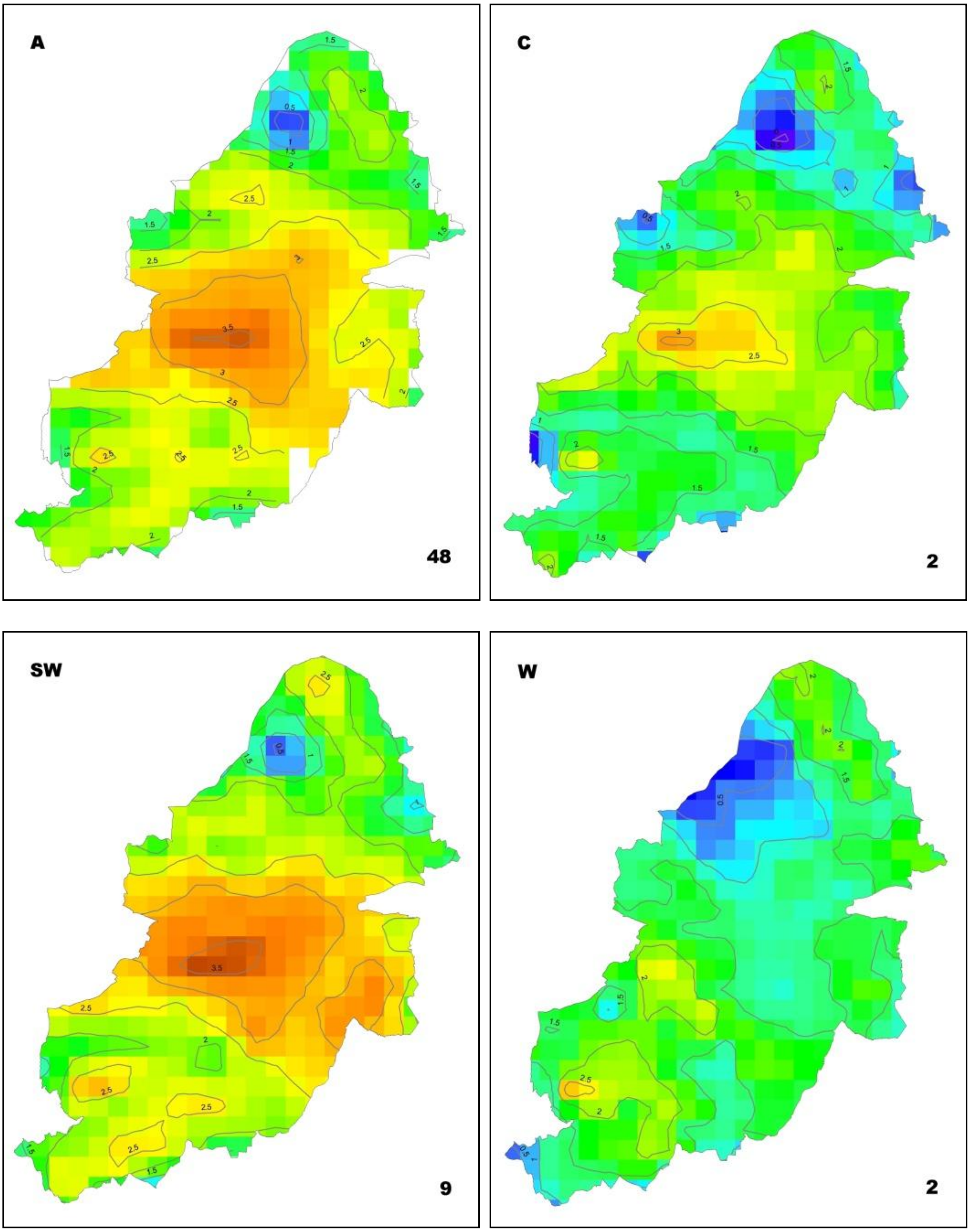
A
48
C
2
SW
9
W
2

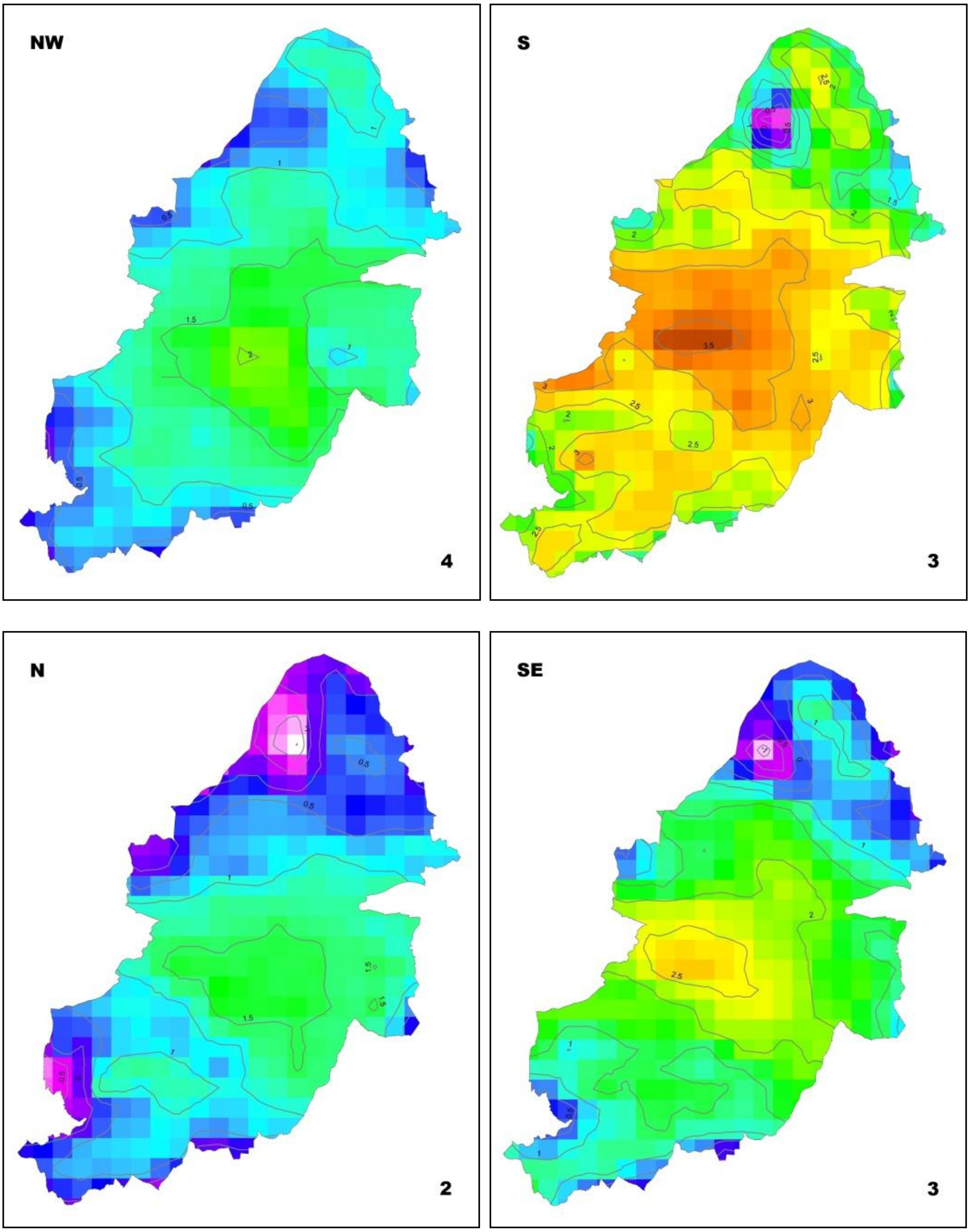
NW
4
S
3
N
2
SE
3

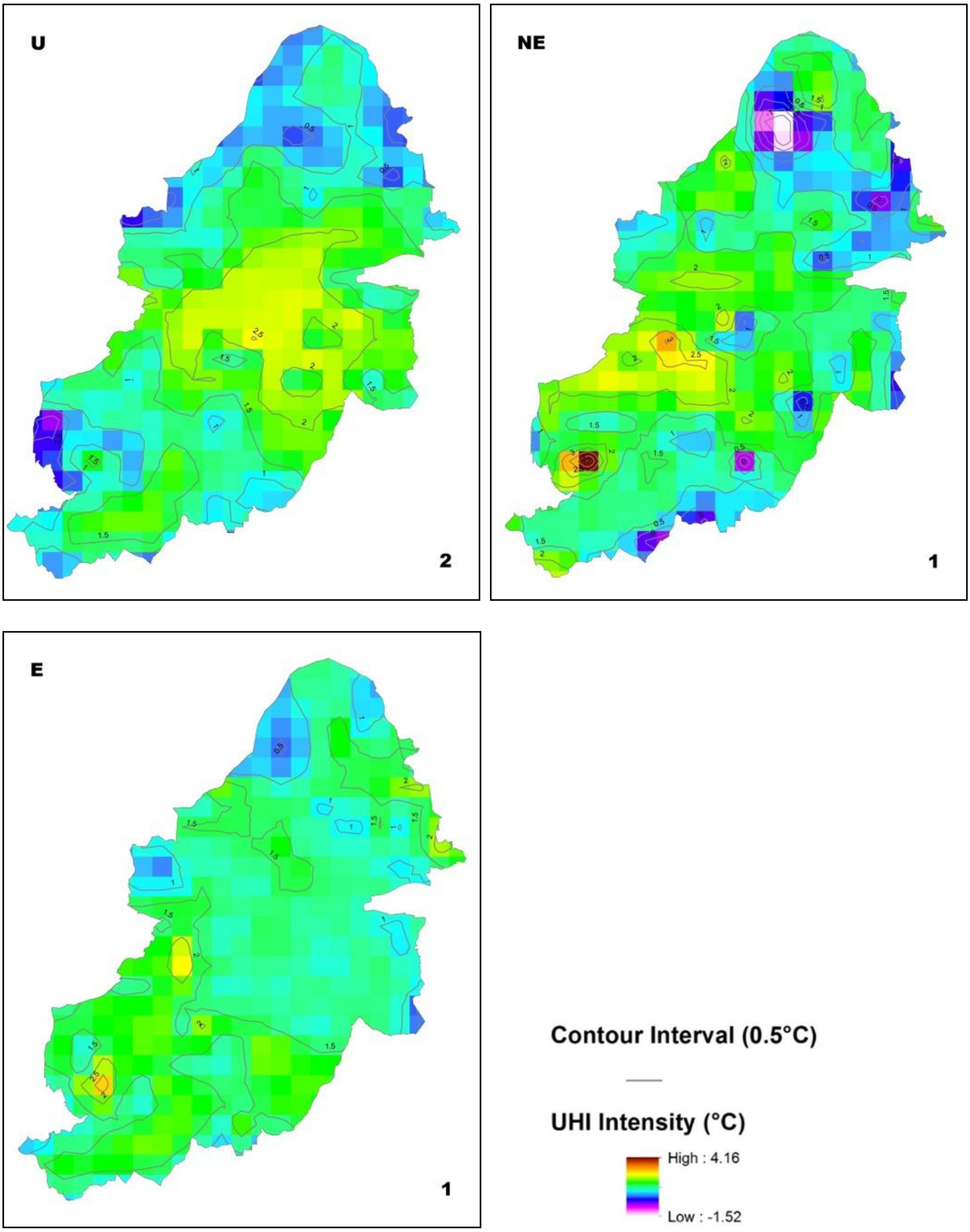

Figure 4. Birmingham's satellite-derived sUHII calculated from the MODIS/Aqua nocturnal LST for eleven LWTs (number at the lower-right corner of each image is the number of days to be averaged; contour lines of sUHII in 0.5 ℃ intervals)

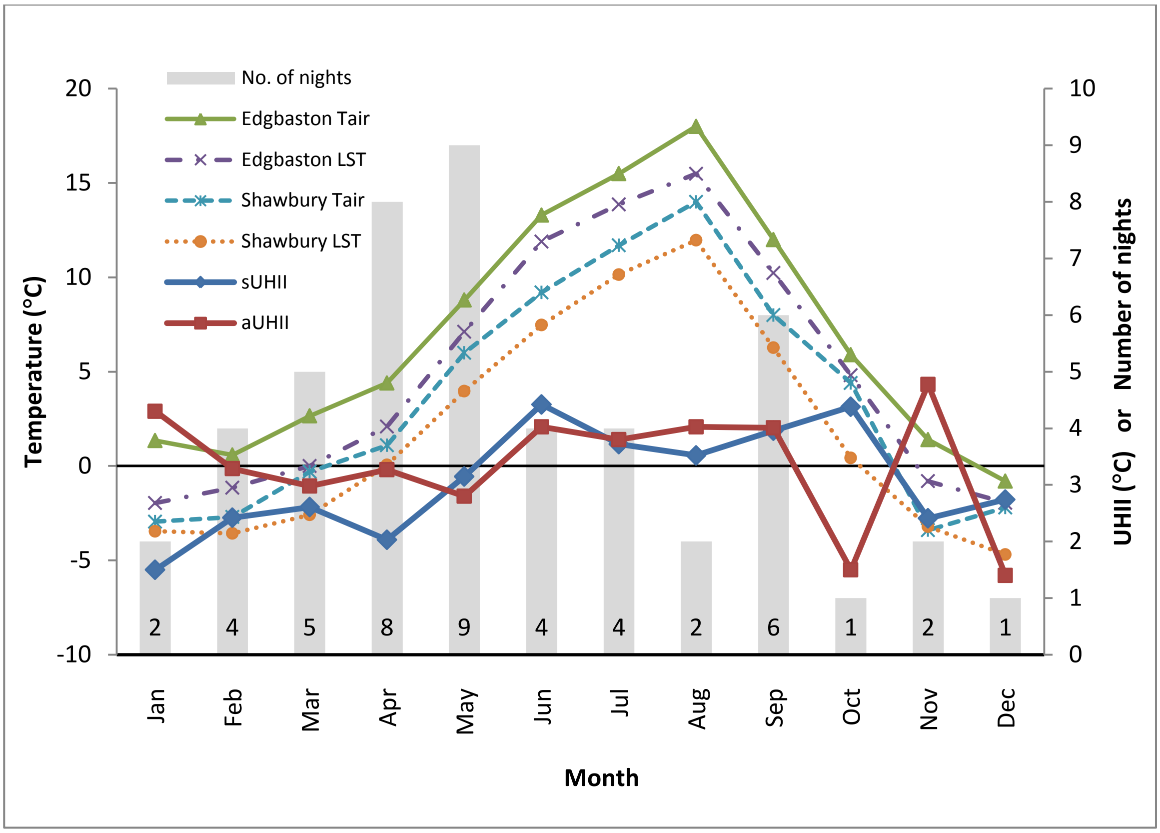

Figure 5. Monthly mean T_{air} (01:30 UTC) and LST at the Edgbaston and Shawbury stations, aUHII and sUHII for the 48 cloudless anticyclonic nights. The bars and the numbers inside indicate the number of nights of each month.

(a)

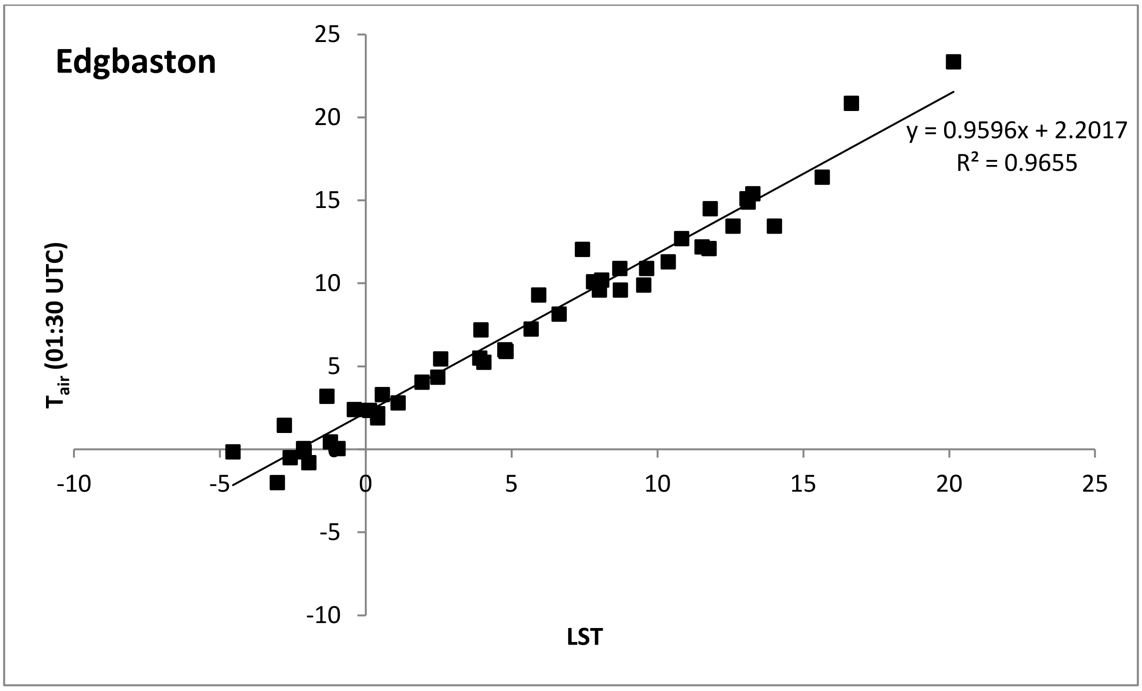
Edgbaston
y = 0.9596x + 2.2017
R^2 = 0.9655
T_{air} (01:30 UTC)
LST
25
20
15
10
5
-5
-10
0
5
10
15
20
25

(b)

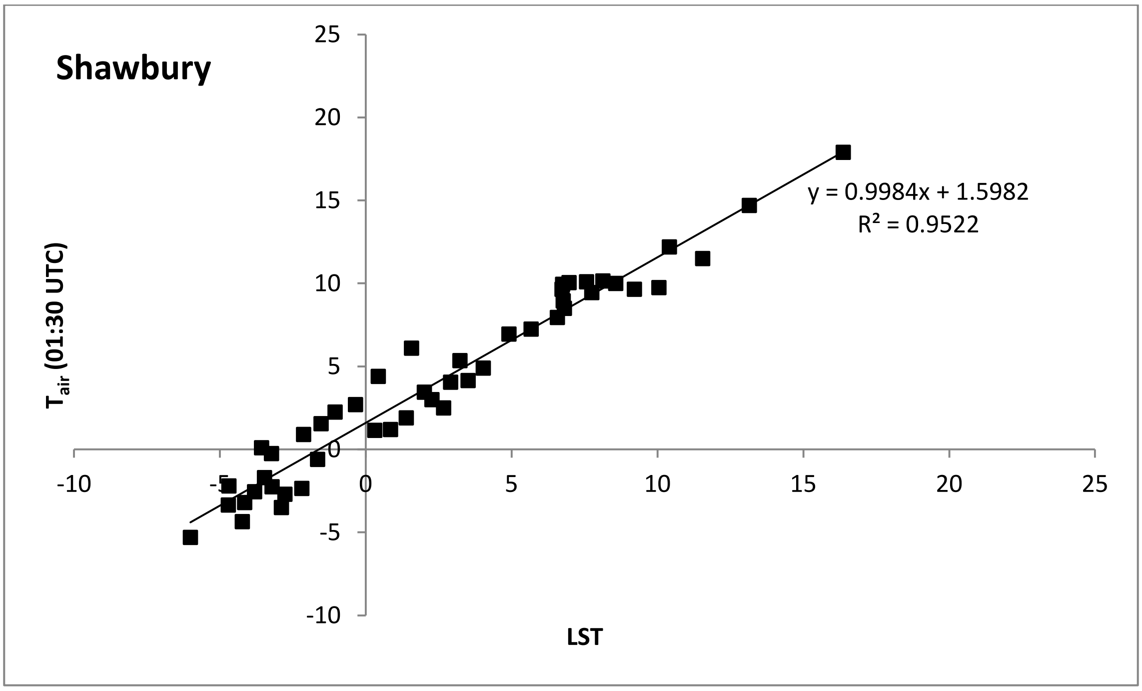
Shawbury
y = 0.9984x + 1.5982
R^2 = 0.9522
T_{air} (01:30 UTC)
LST
25
20
15
10
5
-5
-10
0
5
10
15
20
25

(c)

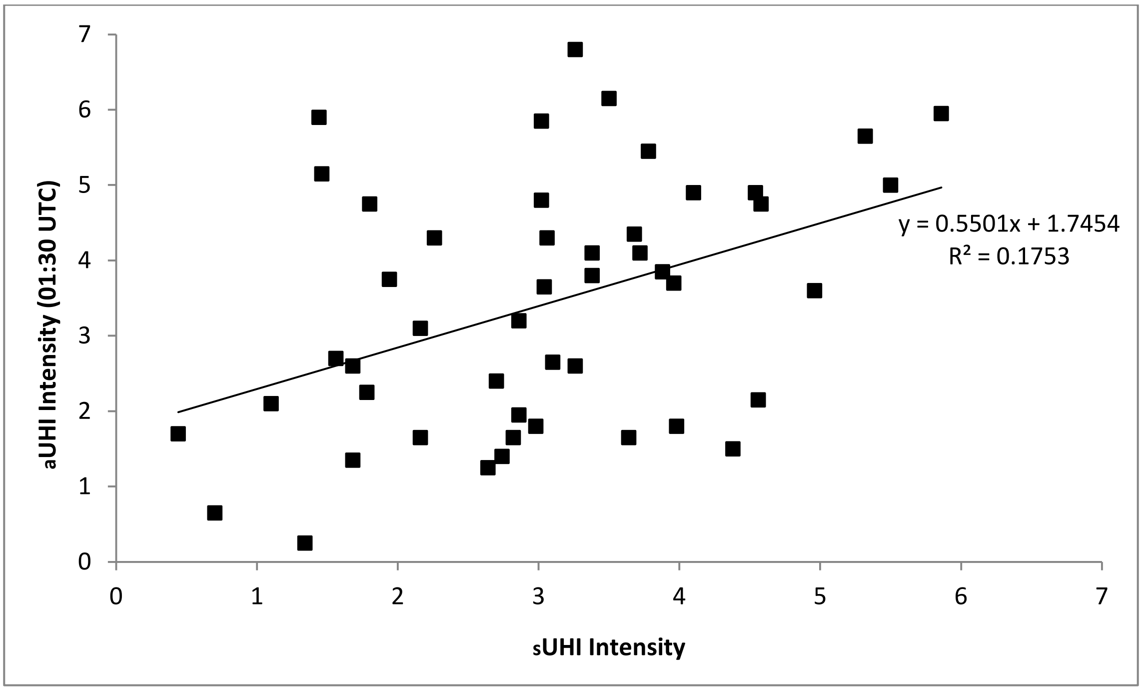

Figure 6. Relationships between nocturnal T_{air} and LST at (a) Edgbaston and (b) Shawbury; (c) Relationship between aUHII and sUHII.

Box 1: Linear relationship between sUHII and aUHII

Assumption 1: We assume that the ground surface of a pixel of the satellite imagery consists of two landuse types: "built-up" (buildings, streets, etc.) and "others" (parks, open ground etc.). We also assume that the satellite-derived land surface temperature of a pixel is a weighted average of two temperatures, one for the "built-up" surfaces, $\mathrm{T}^{(b)}$, and the other for the "others" surfaces, $\mathrm{T}^{(o)}$:

$$\mathrm{LST} = f^{(b)}\mathrm{T}^{(b)} + (1 - f^{(b)})\mathrm{T}^{(o)} \tag{1}$$

where $f^{(b)}$ is the area fraction (%) of the pixel taken by "built-up" landuse type, the superscript $^{(b)}$ denotes "built-up", and the superscript $^{(o)}$ denotes "others". For an urban pixel (e.g. the pixel for the Edgbaston station shown in Fig. 2(a)), Equation (1) becomes

$$\mathrm{LST}_{(u)} = f^{(b)}_{(u)}\mathrm{T}^{(b)} + (1 - f^{(b)}_{(u)})\mathrm{T}^{(o)} \tag{2}$$

and for an rural pixel (e.g. the pixel for the Shawbury station shown in Fig. 2(b)), Equation (1) becomes

$$\mathrm{LST}_{(r)} = f^{(b)}_{(r)}\mathrm{T}^{(b)} + (1 - f^{(b)}_{(r)})\mathrm{T}^{(o)} \tag{3}$$

where the subscript $_{(u)}$ denotes an "urban pixel", the subscript $_{(r)}$ denotes a "rural pixel". It is noted that $f^{(b)}_{(r)}$ can be zero if a rural pixel contains no built-up landuse type (i.e. covered entirely by an open ground). Using the definition of $s\mathrm{UHII} = \mathrm{LST}_{(u)} - \mathrm{LST}_{(r)}$, the subtraction of (3) from (2) yields

$$\mathrm{sUHII} = \alpha \cdot (\mathrm{T}^{(b)} - \mathrm{T}^{(o)}) \tag{4}$$

where, $\alpha = \Delta f^{(b)} = f^{(b)}_{(u)} - f^{(b)}_{(r)}$, interpreted as the difference of "built-up" area fraction between the urban pixel and the rural pixel.

Assumption 2: We further assume that at night, the air temperature measured at an urban weather station, $\mathrm{T}_{\mathrm{air}(u)}$, is in equilibrium with the surface temperature of the "built-up" landuse type, $\mathrm{T}^{(b)}$, i.e.,

$$\mathrm{T}_{\mathrm{air}(u)} = \mathrm{T}^{(b)} \tag{5}$$

and that air temperature measured at a rural weather station, $\mathrm{T}_{\mathrm{air}(r)}$, is in equilibrium with the surface temperature of the "others" landuse type, $\mathrm{T}^{(o)}$, i.e.,

$$\mathrm{T}_{\mathrm{air}(r)} = \mathrm{T}^{(o)} \tag{6}$$

Recalling the definition of $\mathrm{aUHII} = \mathrm{T}_{\mathrm{air}(u)} - \mathrm{T}_{\mathrm{air}(r)}$, substitution of (5) and (6) into (4) yields,

$$\mathrm{sUHII} = \alpha \cdot \mathrm{aUHI} \tag{7}$$

This equation demonstrates that sUHII and aUHII has a linear relationship with a slope of $\Delta f^{(b)}$. In order to match the relationship in Figure 6, Equation (7) can be rearranged as:

$$\mathrm{aUHII} = \frac{1}{\alpha} \cdot \mathrm{sUHI} \tag{8}$$

List of Tables

Table 1. Seasonal mean nocturnal aUHII and (extreme) heat island events, 8th July 2002 to 31st July 2007

Season	Nocturnal aUHII	A. No. nights	B. No. UHI nights >1.5 °C (% of column A)	C. No. extreme UHI nights >5.0 °C (% of column A)
Spring (MAM)	1.4 (1.80)	460	181 (39.3%)	18 (3.9%)
Summer (JJA)	1.7 (1.63)	484	231 (47.7%)	18 (3.7%)
Autumn (SON)	1.5 (1.82)	455	198 (43.5%)	14 (3.1%)
Winter (DJF)	0.8 (1.61)	451	127 (28.2%)	8 (1.8%)
Total	1.4 (1.91)	1850	737 (39.8%)	58 (3.0%)
	(Bracketed values are standard deviations of aUHII)			

Table 2. Summary of nocturnal aUHII, number of nights (frequency percentage) and (extreme) heat island events according to LWTs (1850 nights)

Lamb weather types	Nocturnal aUHII				A. No. nights (% of 1850 nights)	B. No. UHI nights >1.5 ℃ (% of column A)	C. No. extreme UHI nights >5.0 ℃ (% of column A)
	Min	Max	Mean	Std. Deviation			
Anticyclonic [A]	-8.5	7.0	2.5	2.11	391 (21.1%)	255 (65.2%)	47 (12%)
Cyclonic [C]	-1.7	7.3	0.9	1.52	217 (11.7%)	57 (26.3%)	5 (2.3%)
South-westerly [SW]	-2.0	6.7	1.1	1.80	173 (9.4%)	58 (33.5%)	5 (2.9%)
Westerly [W]	-3.3	5.3	1.0	1.66	160 (8.7%)	55 (34.4%)	2 (1.3%)
North-westerly [NW)	-1.7	5.4	1.2	1.40	107 (5.8%)	36 (33.6%)	1 (0.9%)
Southerly [S)	-7.2	7.2	1.1	2.08	104 (5.6%)	32 (30.8%)	4 (3.8%)
Northerly [N]	-1.3	4.9	0.9	1.41	74 (4.0%)	21 (28.4%)	-
South-easterly [SE]	-0.9	5.2	0.9	1.67	54 (2.9%)	14 (25.9%)	1 (1.9%)
Unclassified [U)	-0.9	6.2	2.2	1.93	30 (1.6%)	16 (53.3%)	3 (10%)
North-easterly [NE]	-2.0	4.9	0.7	1.65	25 (1.4%)	5 (20.0%)	-
Easterly [E)	-1.4	4.5	0.6	1.53	25 (1.4%)	5 (20.0%)	-
[A]/[C] hybrids	-11.2	6.5	1.3	1.86	490 (26.4%)	200 (40.8%)	10 (2.0%)